Hypoxia promotes ligand-independent EGF receptor signaling via hypoxia-inducible factor–mediated upregulation of caveolin-1

Yi Wang[a], Olga Roche[a], Chaoying Xu[a], Eduardo H. Moriyama[b,c], Pardeep Heir[a], Jacky Chung[d], Frederik C. Roos[a,e], Yonghong Chen[b], Greg Finak[f,g,h], Michael Milosevic[b], Brian C. Wilson[b,c], Bin Tean Teh[i], Morag Park[f,g,h], Meredith S. Irwin[d,j], and Michael Ohh[a,1]

[a]Department of Laboratory Medicine and Pathobiology, University of Toronto, Toronto, ON, Canada M5S 1A8; [b]Division of Biophysics and Bioimaging and [c]Department of Medical Biophysics, University Health Network, Princess Margaret Hospital, Toronto, ON Canada M5G 2M9; [d]Cell Biology Program, Hospital for Sick Children Research Institute, Toronto, ON, Canada M5G 1L7; [e]Department of Urology, Johannes Gutenberg University, 55101 Mainz, Germany; Departments of [f]Biochemistry, [g]Oncology, and [h]Medicine, McGill University, Montreal, QC, Canada H3A 1A1; [i]Van Andel Research Institute, Grand Rapids, MI 49503; and [j]Department of Paediatrics, Hospital for Sick Children, Toronto, ON, Canada M5G 1X8

Edited by Tak W. Mak, The Campbell Family Institute for Breast Cancer Research, Ontario Cancer Institute at Princess Margaret Hospital, University Health Network, Toronto, ON, Canada, and approved February 7, 2012 (received for review July 28, 2011)

Caveolin-1 (CAV1) is an essential structural constituent of caveolae, specialized lipid raft microdomains on the cell membrane involved in endocytosis and signal transduction, which are inexplicably deregulated and are associated with aggressiveness in numerous cancers. Here we identify CAV1 as a direct transcriptional target of oxygen-labile hypoxia-inducible factor 1 and 2 that accentuates the formation of caveolae, leading to increased dimerization of EGF receptor within the confined surface area of caveolae and its subsequent phosphorylation in the absence of ligand. Hypoxia-inducible factor–dependent up-regulation of CAV1 enhanced the oncogenic potential of tumor cells by increasing the cell proliferative, migratory, and invasive capacities. These results support a concept in which a crisis in oxygen availability or a tumor exhibiting hypoxic signature triggers caveolae formation that bypasses the requirement for ligand engagement to initiate receptor activation and the critical downstream adaptive signaling during a period when ligands required to activate these receptors are limited or are not yet available.

Cellular adaptation to compromised oxygen availability or hypoxia is critically dependent on the activity of heterodimeric hypoxia-inducible factor (HIF) family of transcription factors (1, 2). The catalytic HIFα subunit is oxygen labile by the virtue of the oxygen-dependent degradation (ODD) domain that is targeted for ubiquitin-mediated destruction under normal oxygen tension or normoxia via the von Hippel–Lindau (VHL) tumor suppressor protein-containing E3 ubiquitin ligase, elongins/Cul2/VHL (ECV) (3). Under hypoxia, HIFα escapes the destructive recognition of VHL, recruits p300/Creb-binding protein, and binds to the constitutively expressed and stable HIFβ (also known as "aryl hydrocarbon receptor nuclear translocator," ARNT) to form an active transcription complex (3). HIF engages hypoxia-responsive element (HRE; 5′-RCGTG-3′) within enhancers/promoters to initiate transcription of numerous hypoxia-inducible genes that regulate adaptive responses such as angiogenesis, erythropoiesis, and anaerobic metabolism (2).

Deregulation of HIF has been well documented in common human pathologic conditions such as heart disease, cerebrovascular disease, chronic obstructive pulmonary disease, and cancer (4–6). The extent of HIFα expression, in particular, is correlated with cancer aggressiveness, resistance to radiation and chemotherapy, and poor prognosis (3). Perhaps the most heuristic association is between the loss of VHL and the resulting up-regulation of HIF activity in the development of VHL disease, characterized by tumors in multiple organs, including retinal and cerebellar hemangioblastoma, pheochromocytoma, and clear-cell renal cell carcinoma (CCRCC), the most common form of kidney cancer (3). In addition to causing rare VHL disease-associated tumors, biallelic inactivation of *VHL* is associated with the vast majority of sporadic CCRCC, which typically and expectedly exhibit strong hypoxic profiles.

Caveolin-1 (CAV1) is the major structural component of caveolae, which are 50- to 100-nm flask-shaped vesicular invaginations of the plasma membrane (7). CAV1, through scaffolding domains (CSD), also has been shown to bind several proteins involved in signaling (8). Intriguingly, similar to HIFα, elevated CAV1 expression has been associated with larger tumor size, higher tumor grade and stage, resistance to conventional therapies, and poor prognosis in numerous cancer types in several organs, including colon, liver, stomach, prostate, breast, lung, brain, and kidney (but with the exception of extrahepatic bile duct carcinoma and mucoepidermoid carcinoma of the salivary gland, in which increased CAV1 expression has been correlated with favorable clinical outcome) (9–27). Although these observations suggest a possible correlation between HIF and CAV1, the molecular mechanisms regulating CAV1 expression and CAV1-mediated signaling remain largely unknown.

Results

Hypoxia Promotes CAV1 Expression via HIF. Most of primary CCRCC tumor extracts showed markedly higher expression of CAV1 (12/14) and glucose transporter type 1 (GLUT1) (6/6), a hypoxia indicator, in comparison with matched normal kidney samples (Fig. 1*A* and Fig. S1*A*). *CAV1* mRNA expression, similar to hypoxia-inducible genes *EGLN3*, *CA9*, *VEGFA*, *PDK1*, *GLUT1, HIG2*, and *LOXL2*, was significantly up-regulated in primary CCRCC ($n = 10$) in comparison with the nondiseased renal cortex ($n = 12$) (Fig. 1*B*). The correlation between *CAV1* and the aforementioned HIF target genes, as determined by Pearson's correlation coefficient, was strong ($r > 0.80$) and significant ($P < 0.0001$). Moreover, samples of primary papillary renal cell carcinoma (RCC), the second most common form of kidney cancer, with a strong hypoxic signature displayed increased CAV1 mRNA and protein levels (Fig. S1 *B* and *C*). These results suggest that kidney tumors with elevated hypoxic profiles are associated with increased CAV1 expression.

We next asked whether CAV1 expression is regulated by HIF. 786-MOCK ($VHL^{-/-}$ $HIF1\alpha^{-/-}$) CCRCC cells, which have a high, stabilized level of HIF2α because of the loss of VHL, exhibited elevated CAV1 levels in comparison with isogenically matched 786-O cells stably reconstituted with wild-type VHL (786-VHL) (Fig. 1*C*). Similar results were obtained using a different CCRCC cell line, RCC4 (Fig. S2*A*). Furthermore, 786-VHL cells, as well as

Author contributions: Y.W., E.H.M., M.M., B.C.W., B.T.T., M.P., M.S.I., and M.O. designed research; Y.W., O.R., C.X., E.H.M., P.H., J.C., F.C.R., Y.C., and G.F. performed research; Y.W., O.R., C.X., E.H.M., P.H., J.C., F.C.R., Y.C., G.F., M.M., B.C.W., B.T.T., M.P., M.S.I., and M.O. analyzed data; and Y.W. and M.O. wrote the paper.

The authors declare no conflict of interest.

This article is a PNAS Direct Submission.

[1]To whom correspondence should be addressed. E-mail: michael.ohh@utoronto.ca.

This article contains supporting information online at www.pnas.org/lookup/suppl/doi:10.1073/pnas.1112129109/-/DCSupplemental.

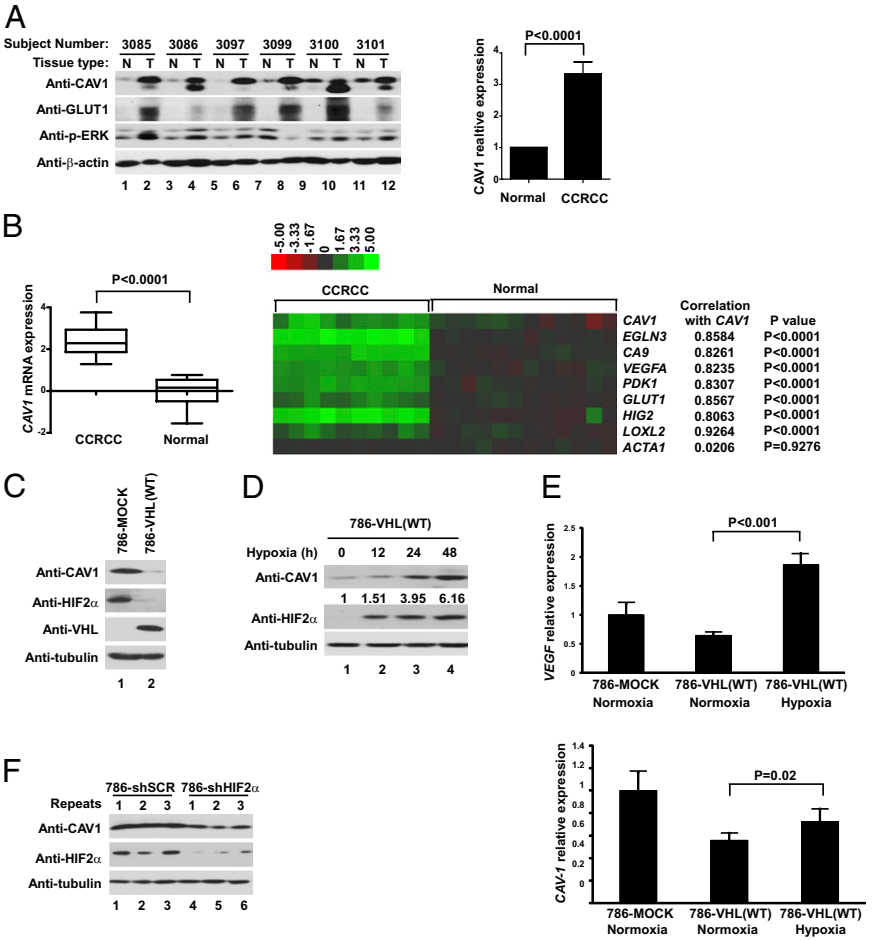

Fig. 1. Hypoxia induces the expression of CAV1 through HIF. (*A*) (*Left*) Cellular extracts generated from primary CCRCC and matched normal kidney samples were resolved by SDS/PAGE and immunoblotted with the indicated antibodies. (*Right*) CAV1 signals were normalized to β-actin as measured by densitometry, and CAV1 signal in normal kidney samples was arbitrarily set at 1. Error bars indicate SD. N, normal tissue; T, tumor. The *P* value was calculated using Student's *t* test. (*B*) (*Left*) Relative gene expression levels of *CAV1* in CCRCC (n = 10) and nondiseased kidney (Normal; n = 12) are shown as a box-whisker plot. Whiskers indicate 0% and 100% quartiles; the boxes indicate 25% and 75% quartiles; the horizontal lines in the boxes indicate the 50% quartile. *P* value was calculated by using a two-sided Welch's *t* test. (*Right*) Relative gene expression levels of *CAV1*, several HIF-target genes, including *EGLN3*, *CA9*, *VEGFA*, *PDK1*, *GLUT1*, *HIG2*, and *LOXL2,* and a negative control *ACTA1* (encoding α-actin) are shown as a heat map. The colorimetric scale indicates relative mRNA expression levels. The correlation between *CAV1* and the indicated hypoxia-inducible genes is represented by Pearson's correlation coefficients. (*C*) Total cell lysates of 786-MOCK and 786-VHL cells were resolved by SDS/PAGE and immunoblotted with the indicated antibodies. (*D*) Equal amounts of total cell lysates generated from 786-VHL cells maintained in hypoxia for the indicated times were separated by SDS/PAGE and immunoblotted with the indicated antibodies. CAV1 signals were normalized to tubulin as measured by densitometry, and the CAV1 signal in 786-VHL lysate without hypoxia treatment (lane 1) was arbitrarily set at 1. (*E*) mRNA was extracted from 786-MOCK and 786-VHL cells maintained in normoxia or hypoxia, and the expression levels of *CAV1* (*Lower*) and *VEGF* (*Upper*) mRNAs were normalized against *U1AsnRNP1* as measured by real-time PCR. *CAV1* and *VEGF* levels in 786-MOCK cells were set arbitrarily at 1. Error bars indicate SD. *P* values were calculated using Student's *t* test. (*F*) Equal amounts of the total cell lysates generated from 786-O cells stably expressing either *HIF2α*-specific shRNA (786-shHIF2α) or nontargeting scrambled shRNA (786-shSCR) were separated by SDS/PAGE and immunoblotted with the indicated antibodies.

other *VHL-null* CCRCC cell lines stably reconstituted with VHL (RCC4-VHL and UMRC2-VHL), but not 786-MOCK cells, maintained under hypoxia showed a time-dependent increase in CAV1 that correlated positively with the induction of HIF2α (Fig. 1*D* and Fig. S2 *B–D*). Similar results were observed in non-CCRCC cell lines that are not associated with *VHL* mutations, including cervical cancer (HeLa), glioma (CNS-1), metastatic breast cancer (MTC-1), epidermoid carcinoma (A431), and murine pro-B (Ba/F3) cell lines, and primary wild-type mouse embryonic fibroblasts (MEFs) (Fig. S2 *E–J*). Consistent with CAV1 protein level, relative *CAV1* mRNA expression was elevated under hypoxia or in the absence of VHL (Fig. 1*E*).

We next asked whether the increased expression of CAV1 under hypoxia or upon the loss of VHL was mediated via HIF. 786-O cells with stable shRNA-mediated knockdown of HIF2α expressed CAV1 levels that were markedly lower than the CAV1 levels of parental 786-O cells expressing nontargeting scrambled shRNA (Fig. 1*F*). Moreover, individual attenuation of either HIF1α or HIF2α in RCC4-MOCK cells down-regulated CAV1 expression, and simultaneous knockdown of HIF1α and HIF2α most profoundly down-regulated CAV1 expression (Fig. S3). Conversely, in HEK293 ($VHL^{+/+}$) cells the ectopic expression of stable HIF1α(P564A) or HIF2α(P531A), in which the proline-to-alanine substitution negates the otherwise prolyl-hydroxylation within ODD that is necessary for VHL recognition, increased CAV1 levels (Fig. S4). Consistent with these findings, the depletion of HIF1α and/or HIF2α in MCF-7 breast cancer cells likewise has been associated with decreased *CAV1* mRNA levels (Gene Expression Omnibus accession number GDS2761) (28). These results demonstrate that hypoxia induces the expression of CAV1, at least in part, via HIF1 or HIF2.

CAV1 Is a Direct Transcriptional Target of HIF via Conserved HRE. The aforementioned expression profiling (Fig. 1*B* and Fig. S1*C*) and quantitative real-time PCR analyses (Fig. 1*E*) strongly suggest that the HIF-mediated regulation of CAV1 occurs, at least in part, at the level of transcription. Consistent with this notion, we identified a conserved HRE within the *CAV1* promoter (Fig. 2*A*) that was capable of binding in vitro-translated radio-labeled HIF1 (HIF1α+ARNT) or HIF2 (HIF2α+ARNT) (Fig. 2*B*). In addition, the levels of HIF1α, HIF2α, and RNA Polymerase II (Pol II) at the endogenous *CAV1* promoter as determined by ChIP were markedly lower in RCC4-VHL and 786-VHL cells than in RCC4-MOCK and 786-MOCK cells (Fig. 2 *C* and *D*). These results demonstrate that HIF1α and HIF2α physically bind the *CAV1* promoter via HRE concomitant with the engagement of Pol II and the induction of *CAV1* transcription.

Loss of VHL Function Is Associated with Increased Caveolae Formation. A major component of caveolae is CAV1. Thus, we asked whether the status of HIF affected caveolae formation by taking advantage of stable 786-O($VHL^{-/-}$; $HIF1\alpha^{-/-}$) subclones expressing various mutant forms of VHL that are either deficient or proficient in degrading HIF2α. VHL-null 786-O and 786-VHL(C162F) (an α domain mutant that has lost the ability to degrade HIFα because

CELL BIOLOGY

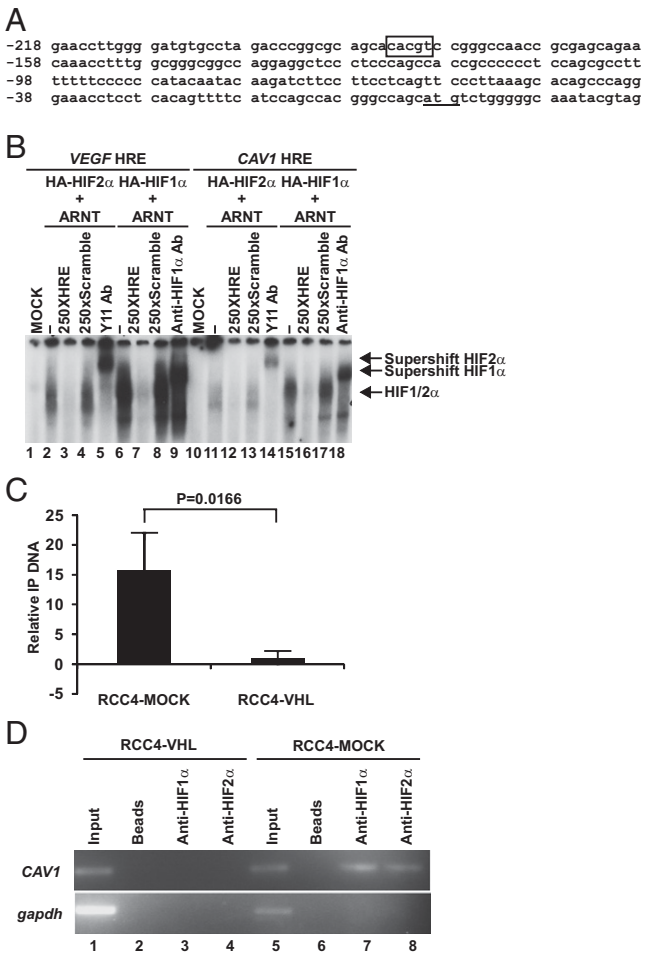

Fig. 2. HIF engagement of HRE on the *CAV1* promoter is associated with increased Pol II recruitment. (*A*) Human *CAV1* promoter sequence showing the conserved HRE (box) and the translation start site (underlined). (*B*) EMSA was performed using ^{32}P-labeled *VEGF* and *CAV1* HRE probes mixed with the indicated in vitro-translated gene products. A 250-fold molar excess of unlabeled wild-type *VEGF* HRE (lanes 3 and 7) or *CAV1* HRE (lanes 12 and 16) was mixed with the reaction mixtures. HIF1 (HA-HIF1α/ARNT) and HIF2 (HA-HIF2α/ARNT) complexes bound to HRE were supershifted with anti-HIF1α (lanes 9 and 18) and anti-HIF2α (lanes 5 and 14) antibodies, respectively. (*C*) Anti-Pol II ChIP analysis was conducted on the endogenous *CAV1* promoter in RCC4-VHL and RCC4-MOCK cells using anti-RNA Pol II antibody. The relative immunoprecipitated (IP) DNA was determined as described in *Materials and Methods*. Error bars represent SDs of indicated IP DNA performed in triplicate in a representative experiment. The *P* value was calculated using Student's *t* test. (*D*) Anti-HIF1α and anti-HIF2α ChIP analysis was performed on RCC4-VHL and RCC4-MOCK cells, and semiquantitative PCR was performed using primers specific for the *CAV1* and *Gapdh* promoters.

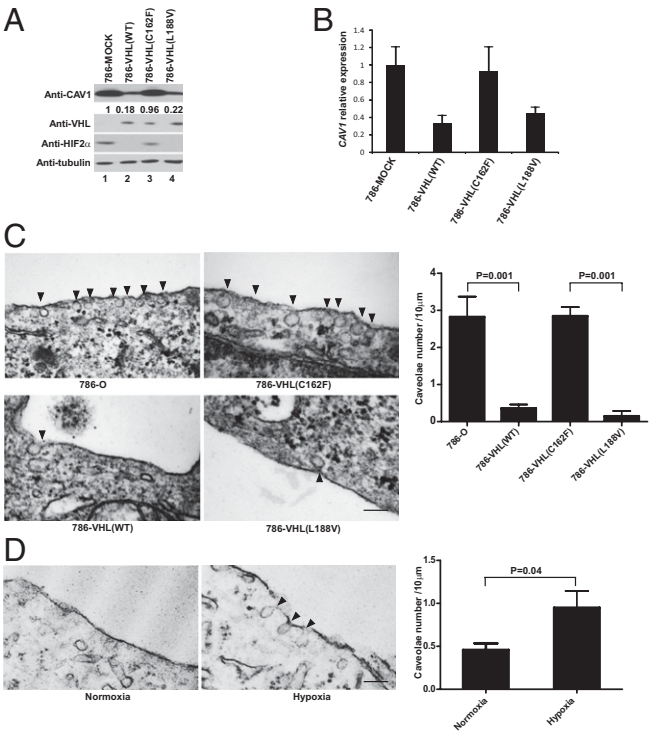

Fig. 3. HIF promotes the formation of caveolae via positive regulation of CAV1. (*A*) Equal amounts of total cell lysates generated from the indicated isogenically matched subclones were resolved by SDS/PAGE and immunoblotted with the indicated antibodies. CAV1 signals were normalized to tubulin as measured by densitometry, and the CAV1 signal in 786-MOCK lysate (lane 1) was set arbitrarily at 1. (*B*) mRNA was extracted from the indicated cells, and the expression level of *CAV1* mRNA was normalized against *U1AsnRNP1* as measured by real-time PCR. The *CAV1* level in 786-MOCK was set arbitrarily at 1. Error bars indicate SD. (*C*) (*Left*) The indicated cells were fixed and visualized by Hitachi H-7000 transmission electron microscopy. (Magnification: 100,000×.) Arrowheads indicate caveolae. (Scale bar.100 nm.) (*Right*) The number of caveolae structures on the cell membrane was quantified by transmission electron microscopy as described in *Materials and Methods*. Error bars indicate SD. *P* values were calculated using Student's *t* test. (*D*) (*Left*) 786-VHL cells maintained in normoxia or hypoxia for 48 h were fixed and visualized by Hitachi H-7000 transmission electron microscopy. (Magnification:100,000×.) Arrowheads indicate caveolae. (Scale bar: 100 nm.) (*Right*) The number of caveolae structures on the cell membrane was quantified by transmission electron microscopy as described in *Materials and Methods*. Error bars indicate SD. *P* values were calculated using Student's *t* test.

of a failure to form the E3 ligase ECV) (29) showed markedly increased CAV1 mRNA and protein levels in comparison with 786-VHL(WT) and 786-VHL(L188V) (a mutant that has retained E3 ligase function to degrade HIFα) (Fig. 3 *A* and *B*) (29). Ultrastructural analysis using transmission electron microscopy showed that 786-O and 786-VHL(C162F) cells exhibited greater numbers of caveolae than did 786-VHL(WT) or 786-VHL (L188V) cells (Fig. 3*C*). Importantly, maintenance of 786-VHL (WT) cells under hypoxia increased the appearance of caveolae (Fig. 3*D*). These results indicate that hypoxia promotes the formation of caveolae via HIF-dependent up-regulation of CAV1.

CAV1 Binds to and Promotes Ligand-Independent Activation of the EGF Receptor. Loss of VHL is associated with increased EGF receptor (EGFR)-mediated signaling, which is thought to contribute to the oncogenic potential of CCRCC (30–32). High concentrations of surface EGFR also have been shown to activate EGFR spontaneously without the participation of ligand (33). Moreover, CAV1 binds to the C terminus of EGFR through the CSD (8), and the cytoplasmic domain of EGFR hasbeen shown to be required for ligand-independent dimer formation (34). Therefore, we asked whether the increased formation of caveolae under hypoxia promoted ligand-independent EGFR clustering and activation on a restricted surface area of caveolae.

Stable shRNA-mediated CAV1 knockdown (786-shCAV1) resulted in reduced levels of caveolae structures (Fig. 4*A*) concomitant with attenuated EGFR phosphorylation in the serum-starved condition (Fig. 4*B*, compare lanes 1 and 3), suggesting that CAV1 promotes EGFR activation in the absence of ligand. In support of this notion, CAV1 coprecipitated EGFR preferentially in the absence of EGF, and the level of EGFR dimerization decreased upon stable shRNA-mediated CAV1 knockdown in 786-O cells (Fig. 4 *C* and *D*). Stable shRNA-mediated CAV1 knockdown in MTC-1 cells likewise decreased EGFR dimerization and phosphorylation (Fig. S5 *A* and *B*). Furthermore, shRNA-mediated CAV1 knock-

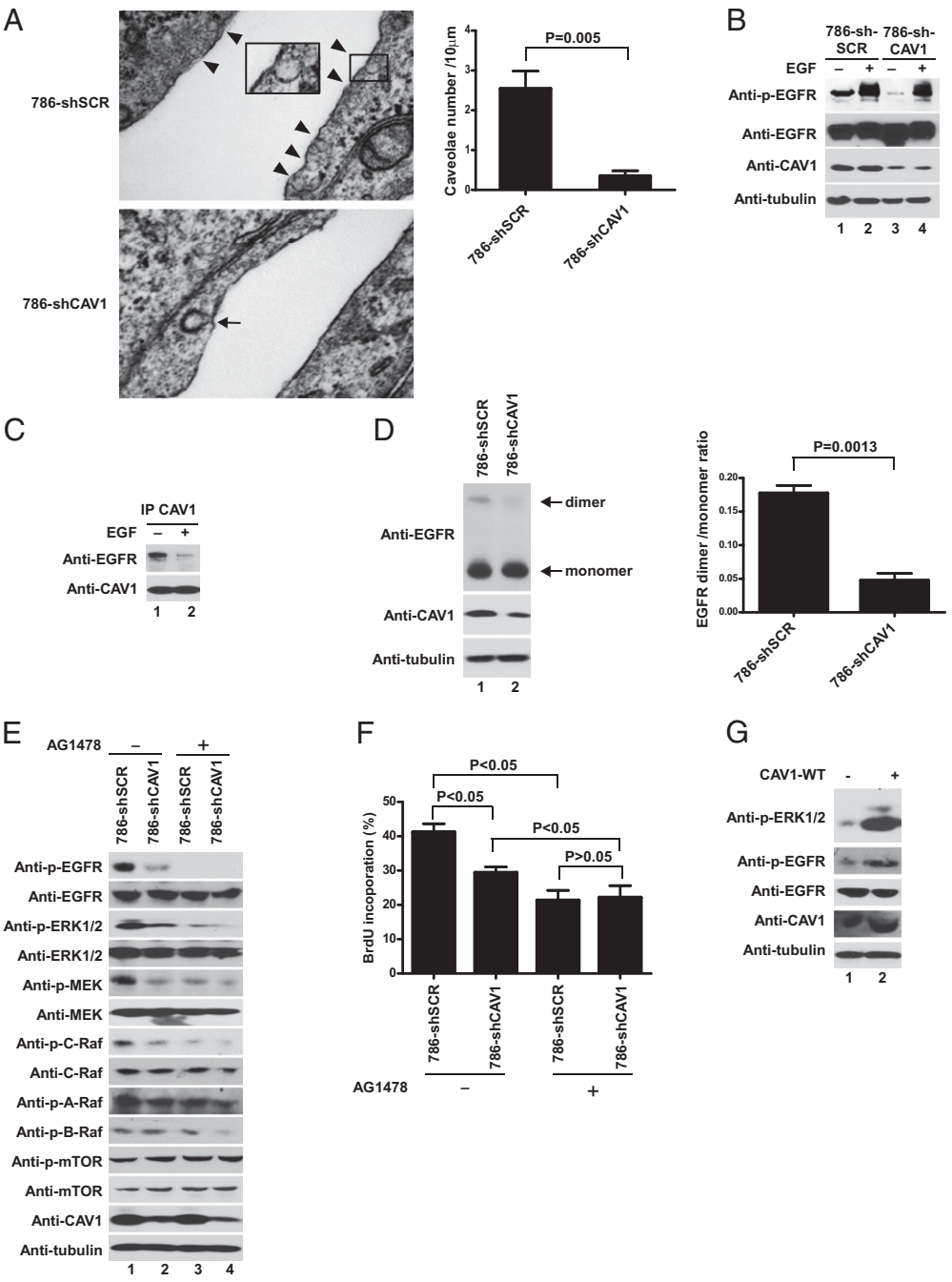

Fig. 4. CAV1 binds EGFR and promotes ligand-independent EGFR phosphorylation and Ras–Raf–MEK–ERK activation. (*A*) (*Left*) 786-shSCR and 786-shCAV1 cells were fixed and visualized by transmission electron microscopy. (Magnification:100,000×.) Arrowheads indicate caveolae; arrow indicates clathrin-coated pit. (Scale bar: 100 nm.) (*Right*) The number of caveolae structures on the cell membrane was quantified by transmission electron microscopy. Error bars indicate SD. The *P* value was calculated using Student's *t* test. (*B*) Equal amounts of total cell lysates generated from serum-starved 786-shSCR and 786-shCAV1 cells that were treated with (+) or without (–) EGF for 5 min were resolved by SDS/PAGE and immunoblotted with the indicated antibodies. (*C*) Serum-starved 786-shSCR cells treated with (+) or without (–) EGF for 5 min were lysed; comparable amounts of total cell lysates immunoprecipitated with anti-CAV1 antibody were resolved by SDS/PAGE and visualized by the indicated antibodies. (*D*) (*Left*) Equal amounts of total cell lysates generated from serum-starved and chemical cross-linked 786-shSCR and 786-shCAV1cells were resolved by SDS/PAGE and immunoblotted with the indicated antibodies. (*Right*) The signals of dimer were normalized to that of monomer as measured by densitometry. Error bars indicate SD. The *P* value was calculated using Student's *t* test. (*E*) 786-shSCR and 786-shCAV1 cells were serum starved overnight with (+) or without (–) AG1478 treatment for 16 h. Equal amounts of total cell lysates separated by SDS/PAGE were immunoblotted with the indicated antibodies. (*F*) BrdU incorporation by 786-shSCR and 786-shCAV1 cells was measured following serum starvation with (+) or without (–) AG1478 treatment for 16 h. Values indicate the mean percentage of BrdU-positive cells in relation to total DAPI-stained nuclei from three independent experiments. Error bars indicate SD. *P* values were calculated using one-way ANOVA followed by a Newman–Keuls post hoc test. (*G*) 786-VHL cells with (+) or without (–) ectopic CAV1 overexpression were serum starved for 16 h. Equal amounts of total cell lysates separated by SDS/PAGE were immunoblotted with the indicated antibodies.

down attenuated the increased EGFR phosphorylation observed in the serum-starved condition upon hypoxic treatment (HeLa cells) or inactivation of VHL (786-O cells) (Fig. S6*A*). Subcellular fractionation indicated that under the serum-starved condition, CAV1 coexists with EGFR in few common fractions and that a fraction of EGFR colocalizes with CAV1 as detected by immunofluorescence microscopy (Fig. S7 *A* and *B*). These results suggest that CAV1 binds and promotes EGFR dimerization and activation in the confined space of caveolae in the absence of ligand.

The downstream Ras–(C)Raf–MEK–ERK signaling and consequential cell proliferation were decreased significantly upon CAV1 knockdown in 786-O cells maintained in serum-free medium [Fig. 4 *E* (compare lanes 1 and 2) and *F*]; this decrease might be attributed, at least in part, to reduced EGFR phosphorylation. In support of this notion, treatment with an EGFR-specific inhibitor, AG1478, attenuated Ras–(C)Raf–MEK–ERK signaling and BrdU incorporation in both serum-starved 786-shSCR and 786-shCAV1 cells (Fig. 4 *E* and *F*). This association also was observed in primary CCRCC specimens where high CAV1 expression generally was associated with increased phosphorylated ERK levels (Fig. 1*A* and Fig. S1*A*). Notably, phosphorylation of A-Raf, B-Raf, and mTOR remained relatively unaffected by changes in CAV1 expression level (Fig. 4*E*). Overexpression (2.2-fold) of CAV1 in 786-VHL cells increased phosphorylated EGFR and ERK levels (Fig. 4*G*). Furthermore, shRNA-mediated CAV1 knockdown attenuated the level of BrdU incorporation observed

in serum-starved 786-O cells maintained under normoxia or hypoxia in comparison with 786-shSRC cells (Fig. S6*B*). CAV1 knockdown likewise reduced the rate of VHL-positive HeLa and MTC cell proliferation under hypoxia (Fig. S8 *D* and *E*). Taken together, these results suggest that, under compromised oxygen availability, the stabilization of HIFα triggers CAV1-dependent cell proliferation and activation of caveolae-sequestered EGFR during limited ligand availability.

CAV1 Overexpression via HIF2 Accentuates Tumor Cell Proliferation. Several lines of evidence have shown that the accumulation of HIF2α upon the loss of VHL has a critical oncogenic role in CCRCC (4, 5, 35, 36). We asked whether CAV1-specific up-regulation via HIF2α had discernable oncogenic property in vivo. 786-O cells stably expressing luciferase-tagged shCAV1 (786-GL-shCAV1) or shSCR (786-GL-shSCR) were injected into the dorsal skin-fold window chamber in SCID mice. The tumor volume over time determined by bioluminescence imaging (BLI) indicated that CAV1 promotes tumor cell proliferation, because the growth rate of 786-GL-shCAV1 xenografts was markedly attenuated in comparison with 786-GL-shSCR xenografts (Fig. S9*A*). In accord, phosphorylated ERK staining was much more prominent in the resected 786-GL-shSCR xenografts than in 786-GL-shCAV1 xenografts (Fig. S9*B*). These results suggest a role for CAV1 overexpression via HIF2α in augmenting tumor cell proliferation in vivo.

Furthermore, CAV1 knockdown in HeLa cells, which express low EGFR levels in comparison with 786-O cells, resulted in a marked down-regulation of PDGF receptor (PDGFR) and type I insulin-like growth factor receptor (IGF-1R) phosphorylation and downstream ERK phosphorylation under serum-starved conditions (Fig. S8*A*). CAV1 knockdown inhibited ligand-independent cell migration and cell invasion as determined by wound healing and Matrigel invasion assays, respectively (Fig. S8 *B* and *C*). These results are consistent with the role of PDGFR and IGF-1R in cell motility (37, 38) and support a role for CAV1 in hypoxia-mediated activation of potentially multiple receptor tyrosine kinases (RTKs).

Discussion

Hypoxia triggers essential physiologic adaptive responses ranging from increased production of oxygen-carrying red blood cells to the formation of new blood vessels and switching cellular energy production from aerobic respiration to anaerobic glycolytic metabolism (32). These and other hypoxia-inducible biological processes are governed principally by HIF transcriptional factor that becomes active upon stabilization of the otherwise oxygen-labile HIFα subunit under hypoxia. Recently, we showed that HIF decelerates clathrin-mediated endocytosis at the early endosome sorting stage and thereby prolongs RTK-mediated signaling to promote cell survival under hypoxia (30, 32). Here we show that CAV1, an integral structural component of caveolae, is a direct target of HIF1 and HIF2 and under hypoxia binds to and promotes ligand-independent activation of EGFR within the substantially smaller surface area of caveolae relative to the plasma membrane.

The observation that CAV1–EGFR interaction is diminished in the presence of ligand is intriguing (Fig. 4*C*) and suggests that CAV1 may not have a significant role in RTK-mediated signaling when the availability of ligand is no longer limited. Consistent with this notion, we found robust and comparable EGFR phosphorylation irrespective of CAV1 expression level in the presence of exogenous EGF (Fig. 4*B*). These observations suggest either that ligand-mediated clustering of EGFR on plasma membrane may hinder trafficking to caveolae or that ligand engagement triggers internalization of EGFR via clathrin-mediated endocytosis and thereby limits the accessibility of EGFR to caveolae. However, in the absence of ligand, some fraction of EGFR in the fluid cell membrane milieu localizes to the caveolae, the formation of which increases markedly under hypoxia. Thus, CAV1-mediated RTK signaling may represent a unique adaptive response triggered under a deleterious situation where the availability of oxygen is compromised and ligands required to activate certain critical adaptive responses are not yet available.

Cancer cells invariably hijack the otherwise normal physiologic responses to hypoxia to potentiate their own survival and growth. HIFα overexpression commonly associated with tumors (by virtue of the general oxygen-sensing pathway in regions of hypoxia or cancer-causing mutations in a growing list of tumor-suppressor genes such as *TSC2*, *PTEN*, *p53*, and *VHL* that bypass the necessity of low oxygen tension to initiate a pseudo hypoxic response) would be predicted to increase CAV1 expression to promote autoactivation of EGFR and other RTKs bound in caveolae. Intriguingly, Martinez-Outschoorn et al. (39) reported that in cancer-associated stromal fibroblasts hypoxia leads to a loss of CAV1 via autophagy, suggesting an indirect negative regulation of CAV1 that may be cell-context dependent. Furthermore, CAV1 was identified originally as an inhibitor of EGFR signaling through receptor sequestration (40, 41). Recently, however, CAV1 has been shown to promote EGFR signaling. For example, under conditions of oxidative stress, CAV1 was shown to transport EGFR to a perinuclear location where EGFR no longer is degraded and remains active (42). CAV1-overexpressing MCF-7 breast cancer cells (MCF-7/CAV1) stimulated with EGF displayed higher EGFR signaling, with enhanced proliferative and motility rates, than seen in MCF-7 parental cells (43). These examples of differential roles of CAV1 in the regulation of EGFR also may suggest the cell context-dependent nature of CAV1 function.

The direct link between CAV1 and HIF presented herein likely explains why, in various tumors including CCRCC, CAV1 overexpression, similar to HIFα, is associated with larger tumor size, higher tumor grade and stage, resistance to conventional therapies, and poor prognosis (10–15, 44). Consistent with this notion, primary CCRCC cells with a strong hypoxic signature exhibited elevated expression of CAV1 and phosphorylated ERK levels, and molecular suppression of CAV1 attenuated Ras–(C)Raf–MEK–ERK signaling, cell proliferation, and migratory capacity in the absence of ligand. Thus, the present study unveils CAV1 as an integral direct component of HIF-mediated signaling in response to tumor hypoxia or pseudohypoxia that transforms cellular architecture to drive receptor-mediated proliferative signaling in the absence of appropriate extracellular cues/ligand (Fig. S9*C*).

Up-regulation of the EGFR signaling pathway has been observed and reported to promote tumorigenesis in CCRCC (45). We show here that HIF-dependent overexpression of CAV1 promotes EGFR signaling in CCRCC. Interestingly, gefitinib, an EGFR-specific inhibitor, inhibited the proliferation of MCF-7/CAV1 breast cancer cells more efficiently than it prohibited the proliferation of MCF-7 parental cells (46). This finding suggests that gefitinib may have beneficial effect on CCRCC displaying a CAV1 overexpression signature. Moreover, combined treatment of metastatic RCC with gefitinib and sunitinib, a multitargeted tyrosine kinase inhibitor of VEGF receptor (VEGFR) and PDGFR, demonstrated efficacy comparable to sunitinib monotherapy with an acceptable safety profile in a Phase I/II clinical trial (47). Notably, sunitinib, a drug approved by the Food and Drug Administration for the treatment of metastatic RCC, has shown significant advantage over IFN-α therapy, the previous first-line therapy for metastatic RCC (48). We show here that CAV1 promotes the activation of other RTKs, such as PDGFR and IGF-1R. Thus, the efficacy of sunitinib for the treatment of metastatic RCC may be caused in part by CAV1 activation of several RTKs involved in the oncogenic processes of CCRCC.

Materials and Methods

Clinical Samples. Institutional review board approval was obtained from each participating institution, and informed consent was obtained from all participants. For preparation of protein extracts, renal tumor tissue was pulverized in a mortar under liquid nitrogen and was suspended on ice in lysis buffer [20 mM Hepes (pH 7.7), 0.2 M NaCl, 1.5 mM $MgCl_2$, 0.4 mM EDTA, 1% Triton X-100, 0.5 mM DTT, 100 μg/mL leupeptin, 100 μg/mL aprotinin, 10 mM benzamidine, 2 mM phenylmethylsulfonyl fluoride, 20 mM β-glycerophosphate, and 0.1 mM sodium-orthovanadate].

Cells. HEK293 embryonic kidney, 786-O ($VHL^{-/-}$; $HIF1\alpha^{-/-}$) CCRCC, HeLa cervical cancer, CNS-1 glioma, MTC-1 metastatic breast cancer, and A431 epidermoid carcinoma cell lines were obtained from the American Type Culture Collection and maintained in DMEM (Gibco) supplemented with 10% (vol/vol) heat-inactivated FBS (Sigma) at 37 °C in a humidified 5% (vol/vol) CO_2 atmosphere. Mouse pro-B Ba/F3 cells were generously provided by Mignon Loh (University of California, San Francisco) (49). These cells were maintained in RPMI-1640 with 10% (vol/vol) FCS (HyClone), penicillin, streptomycin, L-glutamine, and 10 μg/mL mouse IL-3 (Peprotech). Primary MEFs were derived from embryonic day 12.5 wild-type C57BL/6 embryos. 786-O subclones ectopically expressing wild-type hemagglutinin [HA)-VHL(WT)], HA-VHL(C162F), or HA-VHL(L188V) were described previously (50, 51). RCC4 ($VHL^{-/-}$) CCRCC subclones stably expressing HA-VHL (RCC4-VHL) or empty plasmid (RCC4-MOCK) were described previously (52). For hypoxia treatment, cells were maintained at 1% O_2 for the indicated times in a humidified 5% (vol/vol) CO_2 ThermoForma hypoxia incubator at 37 °C.

Additional methodology is described online in *SI Materials and Methods*.

ACKNOWLEDGMENTS. We thank S. Doyle and B. Temkin for assistance with the transmission electron microscopy. This work was supported by Canadian Institutes of Health Research (CHIR) Grant MOP77718 and by Canadian Cancer Society Grant 18460. Y.W. and O.R. are recipients of CIHR postdoctoral fellowships. M.O. holds a Canada Research Chair in Molecular Oncology.

1. Harris AL (2002) Hypoxia—a key regulatory factor in tumour growth. *Nat Rev Cancer* 2:38–47.
2. Semenza GL (2003) Targeting HIF-1 for cancer therapy. *Nat Rev Cancer* 3:721–732.
3. Kaelin WG, Jr. (2002) Molecular basis of the VHL hereditary cancer syndrome. *Nat Rev Cancer* 2:673–682.
4. Kondo K, Kim WY, Lechpammer M, Kaelin WG, Jr. (2003) Inhibition of HIF2alpha is sufficient to suppress pVHL-defective tumor growth. *PLoS Biol* 1:E83.
5. Roberts AM, Ohh M (2008) Beyond the hypoxia-inducible factor-centric tumour suppressor model of von Hippel-Lindau. *Curr Opin Oncol* 20:83–89.
6. Kondo K, Klco J, Nakamura E, Lechpammer M, Kaelin WG, Jr. (2002) Inhibition of HIF is necessary for tumor suppression by the von Hippel-Lindau protein. *Cancer Cell* 1: 237–246.
7. Parton RG, Simons K (2007) The multiple faces of caveolae. *Nat Rev Mol Cell Biol* 8: 185–194.
8. Abulrob A, et al. (2004) Interactions of EGFR and caveolin-1 in human glioblastoma cells: Evidence that tyrosine phosphorylation regulates EGFR association with caveolae. *Oncogene* 23:6967–6979.
9. Tamaskar I, et al. (2007) Differential expression of caveolin-1 in renal neoplasms. *Cancer* 110:776–782.
10. Horiguchi A, et al. (2004) Impact of caveolin-1 expression on clinicopathological parameters in renal cell carcinoma. *J Urol* 172:718–722.
11. Campbell L, Jasani B, Edwards K, Gumbleton M, Griffiths DF (2008) Combined expression of caveolin-1 and an activated AKT/mTOR pathway predicts reduced disease-free survival in clinically confined renal cell carcinoma. *Br J Cancer* 98:931–940.
12. Campbell L, Gumbleton M, Griffiths DF (2003) Caveolin-1 overexpression predicts poor disease-free survival of patients with clinically confined renal cell carcinoma. *Br J Cancer* 89:1909–1913.
13. Joo HJ, Oh DK, Kim YS, Lee KB, Kim SJ (2004) Increased expression of caveolin-1 and microvessel density correlates with metastasis and poor prognosis in clear cell renal cell carcinoma. *BJU Int* 93:291–296.
14. Garcia E, Li M (2006) Caveolin-1 immunohistochemical analysis in differentiating chromophobe renal cell carcinoma from renal oncocytoma. *Am J Clin Pathol* 125: 392–398.
15. Carrion R, Morgan BE, Tannenbaum M, Salup R, Morgan MB (2003) Caveolin expression in adult renal tumors. *Urol Oncol* 21:191–196.
16. Karam JA, et al. (2007) Caveolin-1 overexpression is associated with aggressive prostate cancer recurrence. *Prostate* 67:614–622.
17. Yang G, Truong LD, Wheeler TM, Thompson TC (1999) Caveolin-1 expression in clinically confined human prostate cancer: A novel prognostic marker. *Cancer Res* 59: 5719–5723.
18. Thompson TC (1998-1999) Metastasis-related genes in prostate cancer: The role of caveolin-1. *Cancer Metastasis Rev* 17:439–442.
19. Fong A, et al. (2003) Expression of caveolin-1 and caveolin-2 in urothelial carcinoma of the urinary bladder correlates with tumor grade and squamous differentiation. *Am J Clin Pathol* 120:93–100.
20. Murakami S, et al. (2003) Caveolin-I overexpression is a favourable prognostic factor for patients with extrahepatic bile duct carcinoma. *Br J Cancer* 88:1234–1238.
21. Shi L, Chen XM, Wang L, Zhang L, Chen Z (2007) Expression of caveolin-1 in mucoepidermoid carcinoma of the salivary glands: Correlation with vascular endothelial growth factor, microvessel density, and clinical outcome. *Cancer* 109:1523–1531.
22. Selga E, Morales C, Noé V, Peinado MA, Ciudad CJ (2008) Role of caveolin 1, E-cadherin, Enolase 2 and PKCalpha on resistance to methotrexate in human HT29 colon cancer cells. *BMC Med Genomics* 1:35.
23. Ho CC, et al. (2008) Caveolin-1 expression is significantly associated with drug resistance and poor prognosis in advanced non-small cell lung cancer patients treated with gemcitabine-based chemotherapy. *Lung Cancer* 59:105–110.
24. Ando T, et al. (2007) The overexpression of caveolin-1 and caveolin-2 correlates with a poor prognosis and tumor progression in esophageal squamous cell carcinoma. *Oncol Rep* 18:601–609.
25. Savage K, et al. (2007) Caveolin 1 is overexpressed and amplified in a subset of basal-like and metaplastic breast carcinomas: A morphologic, ultrastructural, immunohistochemical, and in situ hybridization analysis. *Clin Cancer Res* 13:90–101.
26. Yang G, et al. (1998) Elevated expression of caveolin is associated with prostate and breast cancer. *Clin Cancer Res* 4:1873–1880.
27. Burgermeister E, Liscovitch M, Röcken C, Schmid RM, Ebert MP (2008) Caveats of caveolin-1 in cancer progression. *Cancer Lett* 268:187–201.
28. Elvidge GP, et al. (2006) Concordant regulation of gene expression by hypoxia and 2-oxoglutarate-dependent dioxygenase inhibition: The role of HIF-1alpha, HIF-2alpha, and other pathways. *J Biol Chem* 281:15215–15226.
29. Ohh M, et al. (2000) Ubiquitination of hypoxia-inducible factor requires direct binding to the beta-domain of the von Hippel-Lindau protein. *Nat Cell Biol* 2:423–427.
30. Wang Y, et al. (2009) Regulation of endocytosis via the oxygen-sensing pathway. *Nat Med* 15:319–324.
31. Franovic A, et al. (2007) Translational up-regulation of the EGFR by tumor hypoxia provides a nonmutational explanation for its overexpression in human cancer. *Proc Natl Acad Sci USA* 104:13092–13097.
32. Wang Y, Ohh M (2010) Oxygen-mediated endocytosis in cancer. *J Cell Mol Med* 14: 496–503.
33. Sawano A, Takayama S, Matsuda M, Miyawaki A (2002) Lateral propagation of EGF signaling after local stimulation is dependent on receptor density. *Dev Cell* 3:245–257.
34. Yu X, Sharma KD, Takahashi T, Iwamoto R, Mekada E (2002) Ligand-independent dimer formation of epidermal growth factor receptor (EGFR) is a step separable from ligand-induced EGFR signaling. *Mol Biol Cell* 13:2547–2557.
35. Kondo K, Kaelin WG, Jr. (2001) The von Hippel-Lindau tumor suppressor gene. *Exp Cell Res* 264:117–125.
36. Kondo K, et al. (2002) Comprehensive mutational analysis of the VHL gene in sporadic renal cell carcinoma: Relationship to clinicopathological parameters. *Genes Chromosomes Cancer* 34:58–68.
37. Heldin CH, Westermark B (1999) Mechanism of action and in vivo role of platelet-derived growth factor. *Physiol Rev* 79:1283–1316.
38. O'Connor R (2003) Regulation of IGF-I receptor signaling in tumor cells. *Horm Metab Res* 35:771–777.
39. Martinez-Outschoorn UE, et al. (2010) Autophagy in cancer associated fibroblasts promotes tumor cell survival: Role of hypoxia, HIF1 induction and NFκB activation in the tumor stromal microenvironment. *Cell Cycle* 9:3515–3533.
40. Couet J, Li S, Okamoto T, Ikezu T, Lisanti MP (1997) Identification of peptide and protein ligands for the caveolin-scaffolding domain. Implications for the interaction of caveolin with caveolae-associated proteins. *J Biol Chem* 272:6525–6533.
41. Lajoie P, et al. (2007) Plasma membrane domain organization regulates EGFR signaling in tumor cells. *J Cell Biol* 179:341–356.
42. Khan EM, et al. (2006) Epidermal growth factor receptor exposed to oxidative stress undergoes Src- and caveolin-1-dependent perinuclear trafficking. *J Biol Chem* 281: 14486–14493.
43. Agelaki S, et al. (2009) Caveolin-1 regulates EGFR signaling in MCF-7 breast cancer cells and enhances gefitinib-induced tumor cell inhibition. *Cancer Biol Ther* 8: 1470–1477.
44. Tamaskar I, et al. (2007) Differential expression of caveolin-1 in renal neoplasms. *Cancer* 110:776–782.
45. Smith K, et al. (2005) Silencing of epidermal growth factor receptor suppresses hypoxia-inducible factor-2-driven VHL-/- renal cancer. *Cancer Res* 65:5221–5230.
46. Agelaki S, et al. (2009) Caveolin-1 regulates EGFR signaling in MCF-7 breast cancer cells and enhances gefitinib-induced tumor cell inhibition. *Cancer Biol Ther* 8:1470–1477.
47. Motzer RJ, et al. (2010) Phase I/II trial of sunitinib plus gefitinib in patients with metastatic renal cell carcinoma. *Am J Clin Oncol* 33:614–618.
48. Cella D, et al. (2008) Quality of life in patients with metastatic renal cell carcinoma treated with sunitinib or interferon alfa: Results from a phase III randomized trial. *J Clin Oncol* 26:3763–3769.
49. Niemeyer CM, et al. (2010) Germline CBL mutations cause developmental abnormalities and predispose to juvenile myelomonocytic leukemia. *Nat Genet* 42: 794–800.
50. Hoffman MA, et al. (2001) von Hippel-Lindau protein mutants linked to type 2C VHL disease preserve the ability to downregulate HIF. *Hum Mol Genet* 10: 1019–1027.
51. Lonergan KM, et al. (1998) Regulation of hypoxia-inducible mRNAs by the von Hippel-Lindau tumor suppressor protein requires binding to complexes containing elongins B/C and Cul2. *Mol Cell Biol* 18:732–741.
52. Maxwell PH, et al. (1999) The tumour suppressor protein VHL targets hypoxia-inducible factors for oxygen-dependent proteolysis. *Nature* 399:271–275.